

LA-UR-19-31446

Approved for public release; distribution is unlimited.

Title: MIS High-Purity Plutonium Oxide Oxalate Precipitation/Calcination
Product PBO-47-09-012-023: Final Report

Author(s): Veirs, Douglas Kirk
Stroud, Mary Ann
Martinez, Max A.
Carrillo, Alex
Berg, John M.
Narlesky, Joshua Edward
Simms, Luke
Worl, Laura Ann

Intended for: Report

Issued: 2019-11-13

Disclaimer:

Los Alamos National Laboratory, an affirmative action/equal opportunity employer, is operated by Triad National Security, LLC for the National Nuclear Security Administration of U.S. Department of Energy under contract 89233218CNA000001. By approving this article, the publisher recognizes that the U.S. Government retains nonexclusive, royalty-free license to publish or reproduce the published form of this contribution, or to allow others to do so, for U.S. Government purposes. Los Alamos National Laboratory requests that the publisher identify this article as work performed under the auspices of the U.S. Department of Energy. Los Alamos National Laboratory strongly supports academic freedom and a researcher's right to publish; as an institution, however, the Laboratory does not endorse the viewpoint of a publication or guarantee its technical correctness.

MIS High-Purity Plutonium Oxide Oxalate Precipitation/Calcination Product PBO-47-09-012-023: Final Report

Authors:

D. Kirk Veirs
Mary A. Stroud
Max A. Martinez (retired)
Alex Carrillo (retired)
John M. Berg
Joshua E. Narlesky
Luke Simms
Laura Worl

MIS High-Purity Plutonium Oxide Oxalate Precipitation/Calcination Product Product PBO-47-09-012-0239: Final Report

Abstract

A high-purity fuel-grade plutonium dioxide material from the Material Identification and Surveillance (MIS) Program inventory has been studied with regard to gas generation and corrosion in a storage environment. Sample PBO-47-09-012-023 originated from the Hanford continuous oxalate precipitation and calcination process and represents plutonium oxides from multiple processes currently stored in 3013 containers. After calcination to 950°C, the material contained 87.5% plutonium/ameridium with no major impurities. This study followed over time the gas pressure of a sample with nominally 0.5 wt% water in a sealed container with an internal volume scaled to 1/400th of the volume of a 3013 container. Gas compositions were measured periodically over a three year period. The maximum observed gas pressure was 96 kPa. The increase over the initial pressure was primarily due to generation of hydrogen (5.7 kPa) and nitrogen (2 kPa) gas. Oxygen was a minor component of the initial headspace gas and was depleted. At the completion of the study, the internal components of the sealed container did not show significant signs of corrosion.

Contents

Abstract	2
Figures	4
Tables	4
Introduction	5
Material Characterization	5
Experimental Procedure	8
Results	11
Loading.....	11
TGA-MS Results	11
Moisture addition	12
Gas Generation	14
Moisture measurements on unloading.....	14
Corrosion	16
The H ₂ G-value and rate constants	18
Estimation of the amount of moisture on the material during the gas generation study	19
Behavior of NO ₂ and CO ₂	22
Conclusions	22
Acknowledgements	22
References	23
Attachment 1: Gas Generation Partial Pressure Data and Uncertainties in kPa.....	24
Attachment 2: Gas Generation: Total Pressure	25
Appendix 1: Estimating the monolayer coverage	27
Appendix 2: Stopping power ratio	29
Appendix 3: Obtaining G-values and rate constants	30
Appendix 4: Symbols and Conversion Factors	33

Figures

Figure 1. PBO-47-09-012-023 upon arrival at LANL.	5
Figure 2. The calculated specific power of PBO-47-09-012-023 as a function of time from the last measurement date in 1996. The vertical green lines bound the time the sample was in the reactor. .	7
Figure 3. Amount of He evolved from alpha decay from PBO-47-09-012-023 as a function of time (blue line) and the rate of He evolved as a function of time (red line) calculated using the isotopics reported in Table 2 starting from the last measurement date in 1996. The vertical green lines bound the time the sample was in the reactor.....	7
Figure 4. Dissassembled SSR: Conflat container body (A) with conflat flange lid (B), copper gasket (C), inner bucket (D), pressure transducer (E), and a sampling volume between two sampling valves with connection to the gas manifold (F). Inner bucket slides into container body and holds the mataterial.	8
Figure 5. TGA-MS data for the parent material. Mass 17.00 is H ₂ O, Mass 30 is NO and Mass 46 is NO ₂ and Mass 44 is CO ₂	12
Figure 6. Moisture Addition Curve.....	13
Figure 7. Total pressure and He partial pressure (left axis) and partial pressure of gases (right axis) measured using a gas chromatograph as a function of time.	14
Figure 8. Photographs after unloading: a) inner bucket b) bottom of the inner bucket c), d), & e) possible corrosion inner walls of bucket f) g) & h) bottom of bucket that appeared to be covered with debris.	17
Figure 9. The hydrogen partial pressure and the fit to Equation 1.....	18
Figure 10. Comparison of calculated $G(H_2)$ plotted against the number of calculated water monolayers determined in this study with those from previous research.	21

Tables

Table 1. Material Physical Characteristics.....	6
Table 2. The major elemental impurities.	6
Table 3. Isotopic data listed as mass fraction (g/g plutonium). Specific power is reported in mW per gram of material, not per gram of plutonium. The isotopics and specific power were measured on 7/29/1996 on the as received material.	6
Table 4. The dates of activities related to loading the sample and determining the moisture content.....	9
Table 5. Mass of sample and results of calculation of free gas volume.....	11
Table 6. Moisture data summary at loading.....	13
Table 7. Moisture data summary at unloading.....	15
Table 8. The fit parameters and standard errors from the hydrogen generation data	19
Table 9. The amount of water adsorbed on the material, in the gas phase, and decomposed to form H ₂ expressed as moles, grams, and monolayers. Calculations use SSA = 1.3 m ² g ⁻¹ , m _{mat} = 10.0 g and V _{gas} = 4.391 cm ³ . The amount of strongly bound chemisorbed water on the material was assumed to be 1.5 monolayers at all times.	20
Table 10. $G(H_2)$ calculated from the reaction parameters and the estimated moisture content using equation A3-4 assuming radiolytic decomposition of water to form H ₂	21
Table 11. Rate constants calculated from the reaction parameters and the estimated initial rate from the fit (A_0 k_I) assuming surface catalyzed decomposition of water to form H ₂	21

Introduction

The Los Alamos National Laboratory (LANL) Shelf-life Surveillance project was established under the Material Identification and Surveillance (MIS) Program to identify early indications of potential failure mechanisms in 3013 containers.¹ Samples were taken from plutonium processes across the DOE complex. These “representative” materials were sent to LANL to be included in the MIS inventory.² The small-scale surveillance project is designed to provide gas generation and corrosion information of the MIS represented materials under worst-case moisture loadings. This information, in combination with material characterization, allows predictions of the behavior of 3013 packaged materials stored at DOE sites. Pressure, gas compositions, and corrosion were monitored in small-scale reactors (SSRs) charged with nominally 10-gram samples of plutonium bearing materials with nominally 0.5 wt% water, the upper limit allowed by the DOE’s 3013 Standard.¹

This report discusses PBO-47-09-012-023, a high-purity, product-quality plutonium (Pu) oxide material from the MIS Program inventory that originated from the Hanford continuous oxalate precipitation and calcination process converted from material purified in the nitrate/PUREX N-cell. PBO-47-09-012-023 plutonium oxide is representative of oxides generated from the following processes: ²

- Oxalate Process Product at Hanford
- Oxalate Precipitation of Impure Plutonium Nitrate Solutions at Hanford
- Oxalate Precipitation of Pure Mixed Uranium/Plutonium Nitrate Solutions at Hanford
- Impure and Scrap Plutonium Oxides 80–85 wt% from Hanford PFP and 300 Area
- Oxide from PFP NDA Sources at Hanford
- Oxide from Oxalate Precipitation at Savannah River
- Oxide Precipitation from Nitrate Solutions at LANL.



• **Figure 1.** PBO-47-09-012-023 upon arrival at LANL.

Material Characterization

The high-purity fuel-grade plutonium (Pu) oxide material was calcined at 950 °C for 2 hours on August 20, 1997 (prior to calcination a twenty gram sample was removed for later calcination and loading into the small scale reactor). Material characteristics of the material calcined to 950 °C on August 20, 1997 are summarized in Table 1.

Table 1. Material Physical Characteristics

Specific Surface Area (SSA) 5-point ($\text{m}^2 \text{g}^{-1}$)	1.30 ((1.28, 1.32)
Bulk Density (g cm^{-3})	2.436
Tap Density (g cm^{-3})	3.045
Pycnometer Density (g cm^{-3})	10.7 No data available;estimated value based on similar materials

Table 2 summarizes the wt% of key elements as well as any impurity present as 0.01 wt% or greater. Oxygen is not measured and it is assumed to make up the difference between the sum of the listed elements plus plutonium/americiu and 100%. No measurements of soluble species were conducted for this material.

Table 2. The major elemental impurities.

Element	wt%
Calcium	0.0064
Carbon	0.0020
Chloride	.0685-.0893
Iron	0.0163
Magnesium	0.0059
Potassium	0.0098
Sodium	<0.0070
Nickel	0.0128

Data from calorimetry/gamma isotopics for the as-received (AR) material is listed in Table 3. No data is available for the calcined material.

Table 3. Isotopic data listed as mass fraction (g/g plutonium). Specific power is reported in mW per gram of material, not per gram of plutonium. The isotopics and specific power were measured on 7/29/1996 on the as received material.

Isotope	Mass Fraction (g/gPu)	Total Plutonium (calorimetry) (g Pu/g of material)	0.875
Pu-238	0.000792	Specific Power (mW/g of material)	3.143
Pu-239	0.861123		
Pu-240	0.126022		
Pu-241	0.009596		
Pu-242	0.00247		
Am-241	0.004878		

The specific power of as received PBO-47-09-012-023 calculated using the isotopics and purity reported in Table 3 as a function of time from the 7/29/1996 measurement date is shown in Figure 2.

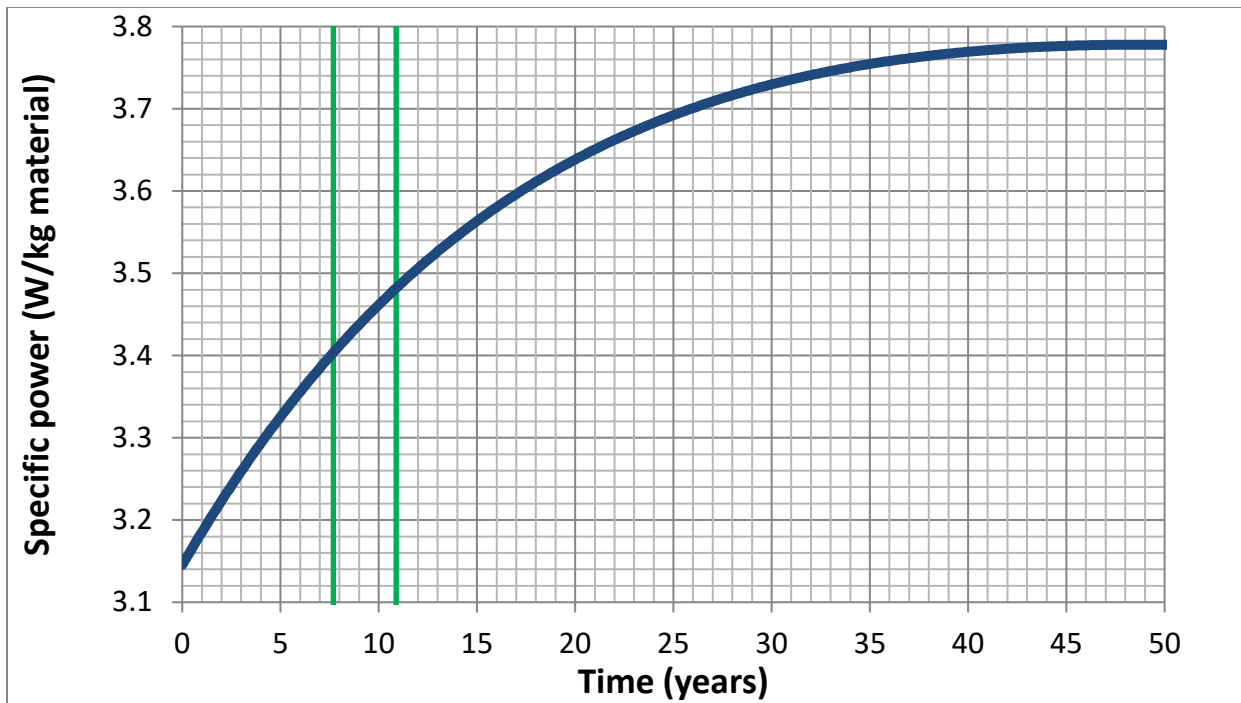


Figure 2. The calculated specific power of PBO-47-09-012-023 as a function of time from the last measurement date in 1996. The vertical green lines bound the time the sample was in the reactor.

Figure 3 provides information on He evolution calculated using the isotopics and purity reported in Table 3 as a function of time for as received PBO-47-09-012-023.

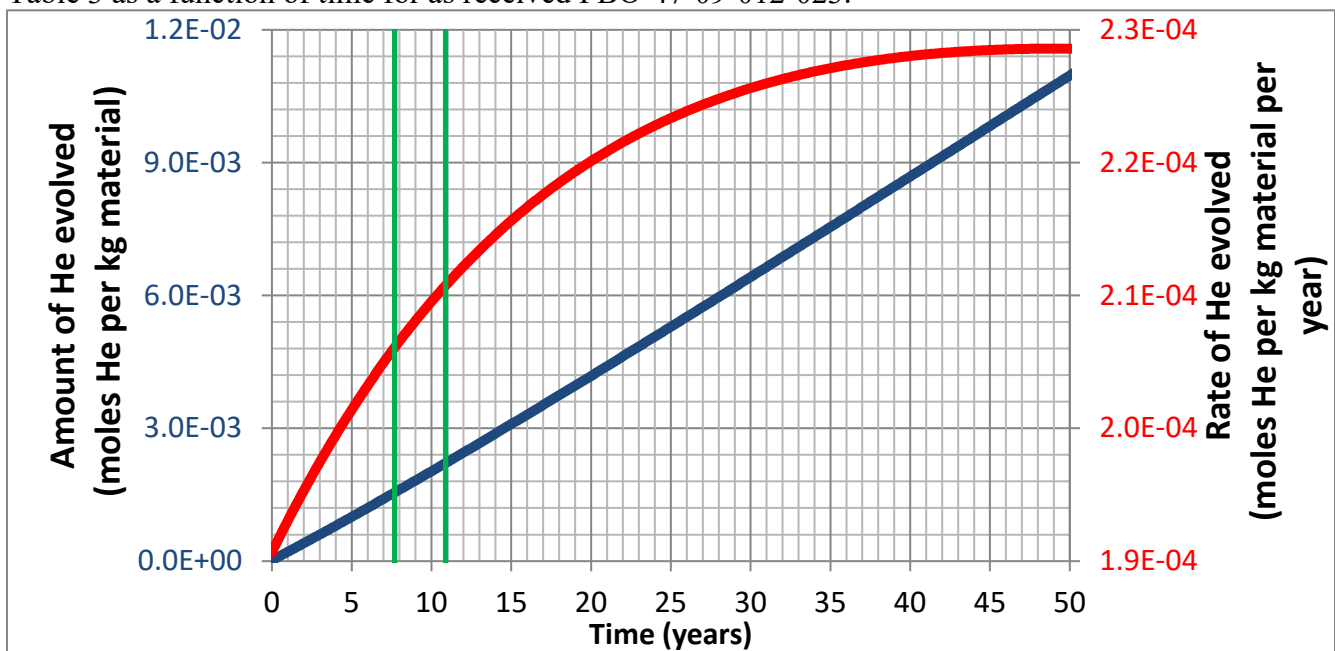


Figure 3. Amount of He evolved from alpha decay from PBO-47-09-012-023 as a function of time (blue line) and the rate of He evolved as a function of time (red line) calculated using the isotopics reported in Table 2 starting from the last measurement date in 1996. The vertical green lines bound the time the sample was in the reactor.

Experimental Procedure

The design of the small-scale reactor (SSR) system has been described previously.³ The container's nominally five cm³ internal volume is scaled to $\sim 1/400^{\text{th}}$ of the inner 3013 storage container. The material of construction of the SSR is 304L stainless steel. The SSR consists of a container body⁴ welded into a Conflat flange and a lid consisting of a Conflat flange with tubing attachments for connections to a pressure transducer and a gas manifold. An inner bucket is used to hold material and is inserted into the container body during the loading activities. The inner bucket allows the fine plutonium oxide powder to be handled with minimal or no spillage. A low-internal-volume pressure transducer and associated low-volume tubing is attached to the lid. Small-scale reactors have interchangeable parts with varying volumes. For this study, a Type H container with a total internal volume of 5.326 cm³ was used.⁴ The gas sampling volume located between two sampling valves, 0.05 cm³ ($\sim 1\%$ of the SSR volume), allows gas composition to be determined with minimal effect on the internal gas pressure. A disassembled SSR is shown in Figure 4.

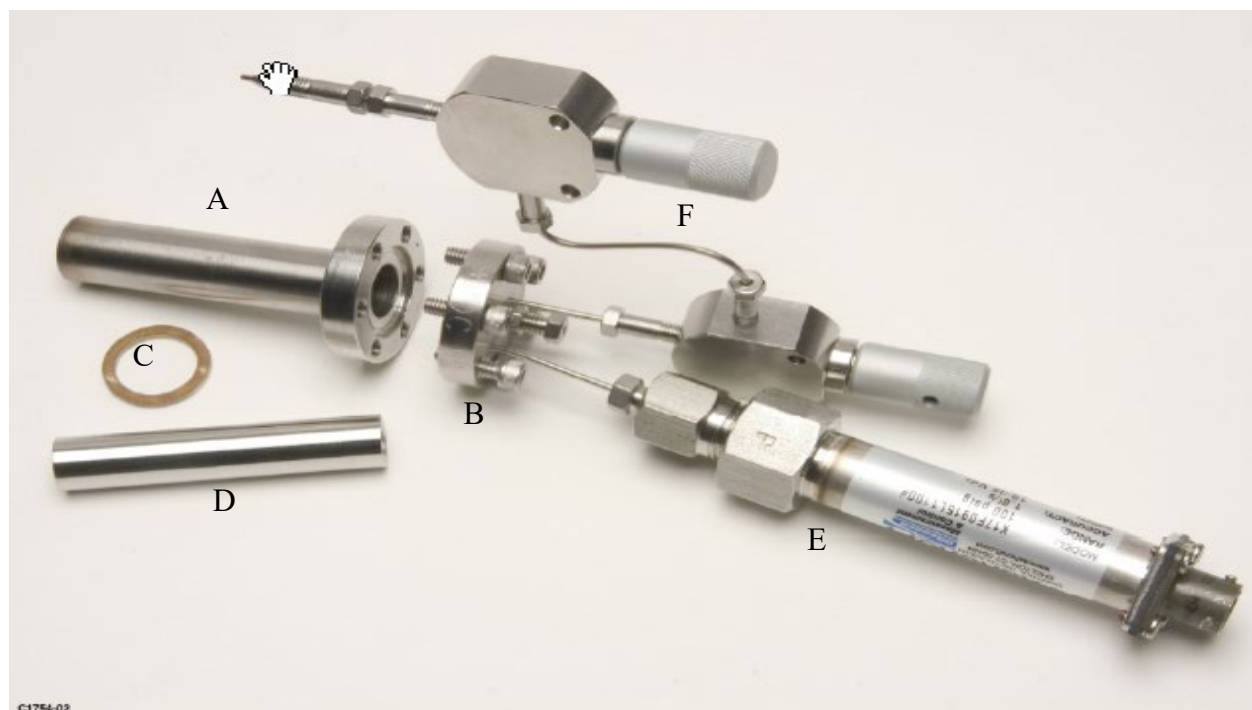


Figure 4. Disassembled SSR: Conflat container body (A) with conflat flange lid (B), copper gasket (C), inner bucket (D), pressure transducer (E), and a sampling volume between two sampling valves with connection to the gas manifold (F). Inner bucket slides into container body and holds the material.

Gas generation is to be characterized for each MIS represented material at the bounding moisture content of 0.5 wt%. The procedure to achieve 0.5 wt% moisture included (1) estimating the moisture content of the material as it was received for small-scale loading and (2) adding sufficient water to bring the total to 0.5 wt%. The moisture content of the material was estimated by weight loss upon heating to 200 °C (LOI-200 °C) of a one gram sample that was cut from the parent lot at the same time as the 10 g small-scale sample. The LOI-200 °C samples were placed in a glass vial which remained in the glove box line with the small-scale sample until the LOI-200 °C measurement was performed, typically one day or less after the sample split and just prior to SSR loading. LOI-200 °C

involved heating nominally one gram of the material for 2 hours at 200 °C, cooling the material for 10 minutes and determining the mass difference of the material before and after heating. The mass loss observed was attributed to adsorbed water. It was assumed that the LOI-200 °C material contained an additional ~1 monolayer equivalent of water, approximately 0.03 wt% for this material, as hydroxyls or chemically adsorbed water which was not removed by heating to 200 °C.⁵ The amount of water to be added to achieve 0.5 wt% total moisture was calculated as the difference between 0.5 wt% and the sum of the adsorbed water determined by LOI-200 °C and the chemically adsorbed water assumed to be 0.03 wt%. In addition, a sample from the parent was split and placed in a glass vial inside of a hermetically sealed container (Swagelok). The water content of this sample was determined by Thermal Gravimetric Analysis-Mass Spectroscopy (TGA-MS). TGA-MS is inherently more accurate than LOI-200 °C, although there can be errors associated with this method due to handling and excessive times before the sample is run.

In this case, several deviations to the desired timing occurred. The timing that the split from the parent lot, PBP40709-SUR, was calcined, samples split from it, when the SSR was loaded, and when LOI-200 °C and TGA-MS were run are detailed in Table 4.

Table 4. The dates of activities related to loading the sample and determining the moisture content.

Date	PBP40709-SUR	SSR142	SSR142S1	SSR142S2	SSR142S3	SSR142S4
3/31/2004	Calcined – 1.65 wt% loss					
4/1/2004		Split -10.00 g	Split – 0.32 g	Split – 0.30 g	Split – 0.31 g	Split – 1.00 g
4/5/2004						LOI – 200 0.05 wt%
4/7/2004		Moisture added 0.47 wt%				
4/7/2004		Sample placed in reactor				
8/30/2006			TGA-MS run Not analyzed			
2/22/2007				TGA-MS run 0.13 wt% water		
6/18/2007		SSR removed				
6/19/2007		RH sensor placed				

The procedure to add moisture is described briefly. A ten-gram sample of calcined PBP40709SUR material was placed on a balance in a humidified chamber. Weight gain was recorded as a function of time. The sample was then placed into an SSR. The glove boxes used for loading and surveillance were flushed with He, resulting in a glove box atmosphere of mainly He with a small amount of air.

Transfer time from the balance where the final mass measurement is made to when the SSR was sealed was approximately 90 seconds. While a moisture loss is typically expected in a dry glove box during transfer, the glove box atmosphere of 9% RH may have resulted in less moisture loss. The 9% glove box RH was due to inadvertently leaving a heater powered in the moisture loading chamber overnight.

The sealed SSR was placed in a heated sample array maintained at 55 °C for 1169 days. Gas samples of fifty microliter (~1.1 % of the headspace gas per sample) were extracted periodically through a gas manifold and analyzed using an Agilent 5890 GC (gas chromatograph) calibrated for He, H₂, N₂, O₂, CO₂, CO and N₂O. Water vapor was not measured in these gas samples. The pressure and array temperature was recorded every fifteen minutes. The pressure data was reduced to weekly average values reported here. Gas composition was determined at least annually.

At the termination of the experiment, a final GC gas sample was taken, and the SSR was removed from the array and allowed to cool to glove box temperature for 19 hours. The SSR lid was removed and a new lid containing a relative humidity sensor was placed on the container. This took one minute in the glove box with 0.4% RH. After allowing 4.5 hours for the system to equilibrate, the relative humidity and temperature in the container were measured using a Vaisala HMT330 sensor and readout. The material was then removed from the container and the moisture content in the material was determined by performing LOI-200 °C.

Results

Loading

A 20 g sample split from the AR material labeled PBP40709-SUR was calcined to 950 °C for two hours on 3/31/04. A ten-gram split from this sample was selected for loading into the SSR. The mass of the sample prior to moisture loading, m_{mat} , the volume the material occupies calculated from m_{mat} and the pycnometer density, V_{mat} , and the calculated free gas volume within the SSR, V_{gas} , during the gas generation study are given in Table 5.

Table 5. Mass of sample and results of calculation of free gas volume.

Mass of sample m_{mat}	Volume of material V_{mat}	Volume of SSR V_{SSR}	Free gas volume V_{gas}
10.00 g	0.94 cm ³	5.326 cm ³	4.39 cm ³

TGA-MS Results

TGA-MS data for SSR142S2, calcined to 950 °C on 3/31/2004 and TGA-MS run on 2/22/2007, are shown in Figure 5. TGA traces and MS traces for channels that were above background are illustrated. Total moisture content was determined to be 0.13 wt%. Carbon dioxide and NO were the primary volatile from 200 °C to 400 °C. NO is the primary MS fragment from NO₂. These components were 0.214 wt% and 0.072 wt% respectively. Calcination to 950 °C would have removed these adsorbed gases, so they were formed within the sealed Swagelok container over the ~3 years between when the sample was split from the calcined parent to when the TGA-MS was run. This is inconsistent with the carbon and nitrogen content of the parent material after calcination to 950 °C. It is possible that these components were formed primarily from radiolysis of the plastic cap of the primary glass vial containment during the ~3 years the sample was stored. The material was in direct contact with the plastic. It is also possible that the bulk of the observed water was also formed from radiolysis of the plastic cap.

Mass 16 (oxygen) is seen as the yellow curve. It is unusual to see mass 16 ion current this low in the TGA-MS instrument used for this measurement. Normally, a very small amount of air leaks into the inert flowing gas in this instrument and the mass 16 peak is too large to be useful. This does not affect the validity of the mass loss or the other ion current measurements. In this case, the mass 16 ion current is low enough to see peaks due to fragmentation patterns. The mass 16 peaks are assigned to fragmentation of CO₂ and H₂O based on correlation.

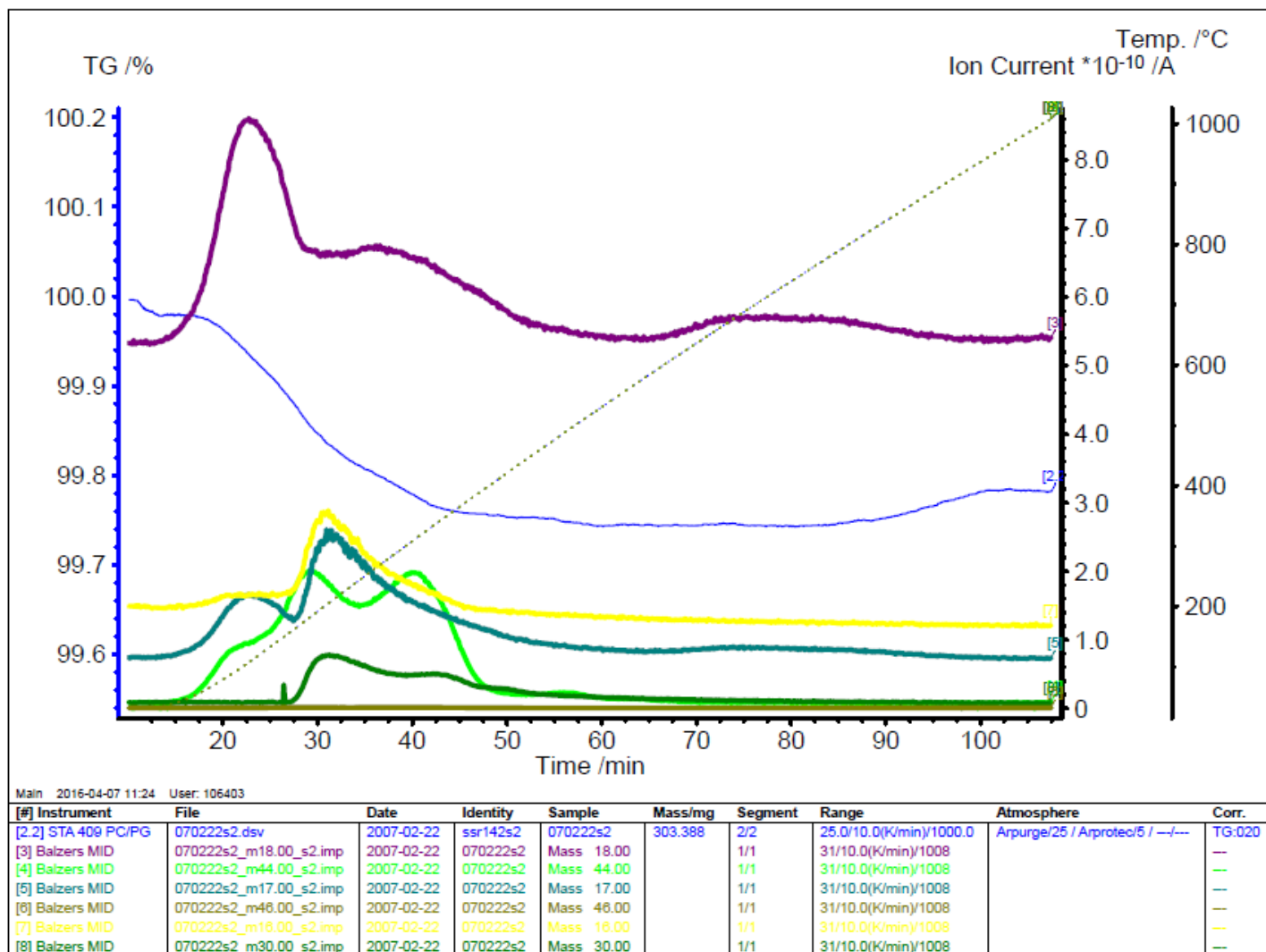


Figure 5. TGA-MS data for the parent material. Mass 17.00 is H₂O, Mass 30 is NO and Mass 46 is NO₂ and Mass 44 is CO₂.

Moisture addition

The measurements and assumptions used to calculate the moisture content at the time of loading are summarized in Table 6. The best value for the moisture content at loading is 0.50 wt% as given in Table 6 line 13, Estimated Total Moisture in loaded sample (using LOI).

Table 6. Moisture data summary at loading.

	Parameter	Value	Units
1	Most recent Calcination Date	3/31/04	
2	Loading Date	4/7/04	
3	Unloading Date	6/18/07	
4	Initial sample weight (m_{mat})	10.00	g
5	Initial Moisture (Total) by TGA-MS	NA	wt%
6	Initial Moisture (Weakly bound) by LOI-200 °C	0.05	wt%
7	Estimated additional (chemisorbed) moisture present – 1.0 ML	0.03	wt%
8	Total Moisture added	0.47	wt%
9	Relative Humidity in glove box during loading	9.0/24.8	% / °C
10	Estimated moisture loss during loading (90 seconds)	0.05	wt%
11	Estimated Weakly Bound Moisture in loaded sample (using LOI) = Line 6 +Line8 -Line 10	0.47	wt%
12	Estimated Total Moisture in loaded sample (using TGA-MS) = Line 5 + Line 8 +Line 10	NA	wt%
13	Estimated Total Moisture in loaded sample (using LOI) = Line 6 +Line7 +Line 8-Line 10	0.50	wt%

The moisture uptake as a function of exposure time to the high humidity atmosphere in the humidified chamber is plotted in Figure 6. The increase in mass is attributed to water adsorption by the material. The estimated sample loss during transfer was reduced from 0.05 wt% per 45 seconds to 0.05 wt% per 90 seconds due to the 9% RH glove box environment.

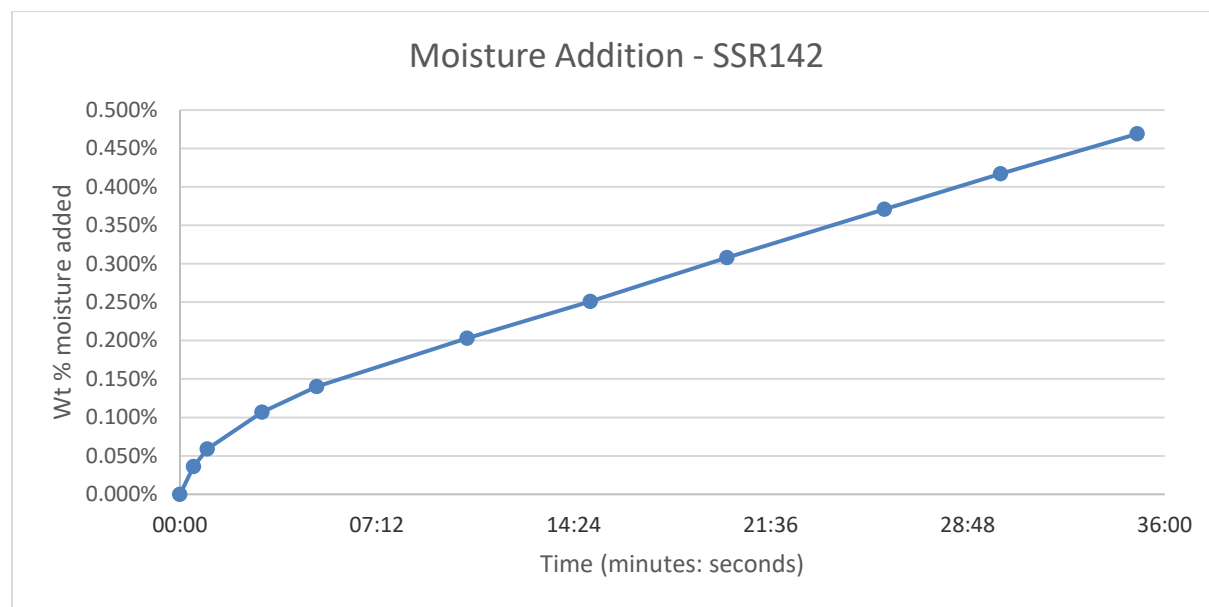


Figure 6. Moisture Addition Curve

Gas Generation

The total pressure in SSR142 as a function of time, as well as the partial pressure of several gasses, is shown in Figure 7. Detailed information on gas composition and uncertainties is in Attachment 1 and on pressure in Attachment 2.

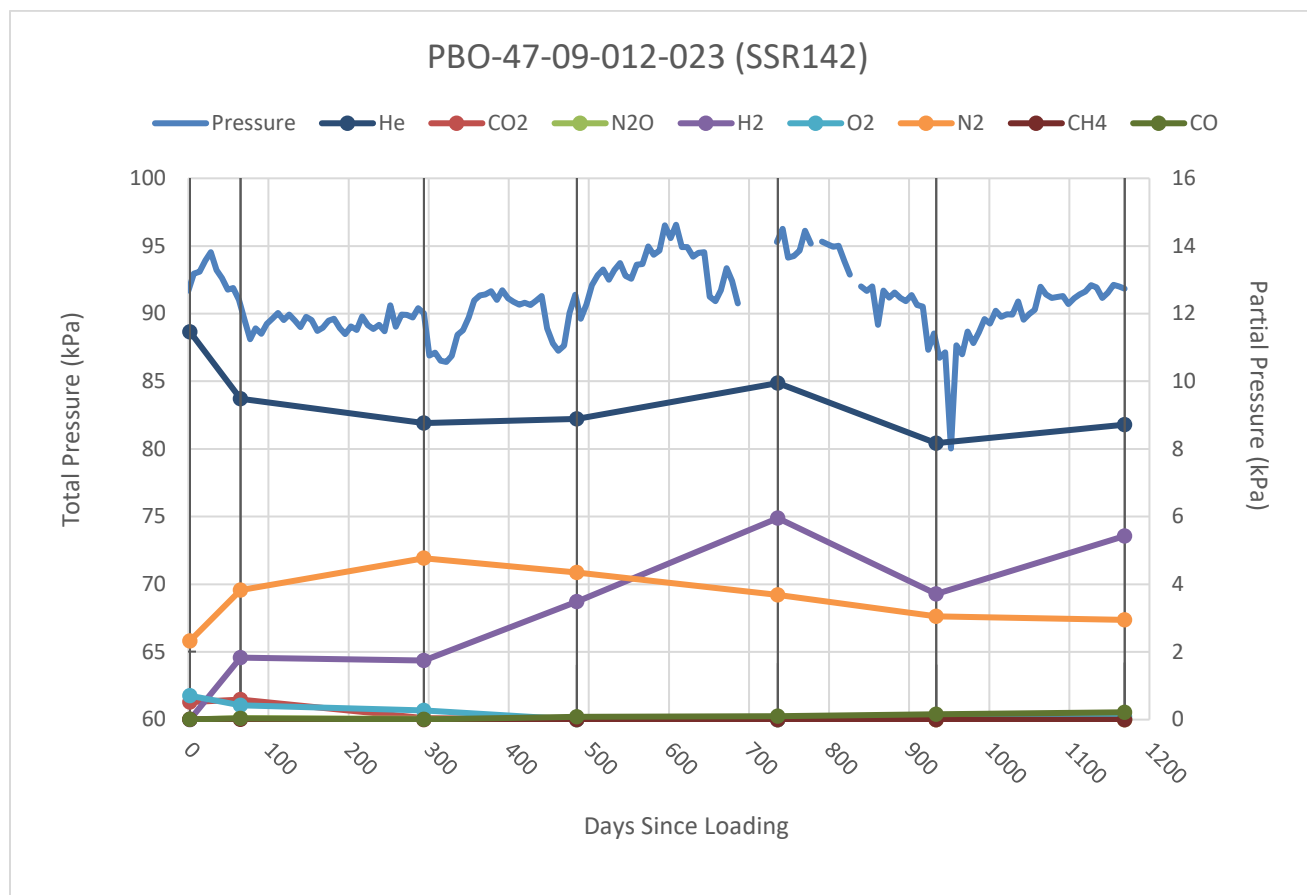


Figure 7. Total pressure and He partial pressure (left axis) and partial pressure of gases (right axis) measured using a gas chromatograph as a function of time.

While the total pressure fluctuated between a low of 80 kPa to a high of 97 kPa over the course of the experiment, the initial, final, and average pressure were all 91 kPa. Nitrogen had an initial pressure of 2.2 kPa and increased to a pressure of 4.6 kPa after 294 days and then displayed a downward trend for the rest of the timeframe. Oxygen had an initial value of 0.7 kPa. Initial N₂ results suggest the oxygen was from air. Oxygen levels decreased to zero between 50 and 300 days. Hydrogen partial pressure increased slowly over the first 736 days reaching a max pressure of 5.7 kPa. However, this maximum corresponded to the unexplained high value in the He partial pressure. A value of 5.2 kPa was detected at the end of the experiment. CO₂, N₂O, O₂, CH₄, and CO did not contribute significantly to the total pressure of SSR 142.

Moisture measurements on unloading

The SSR was removed from the heated array and placed in a holder to cool for 19 hours. The lid was removed and within one minute it was replaced with a lid modified to hold a RH sensor. After

allowing approximately 4.5 hours for the system to equilibrate, the relative humidity and temperature in the container were measured using a Vaisala HMT330 sensor and readout.

The moisture content in the material at unloading was estimated using two approaches – one using LOI at unloading and one using RH at unloading. The LOI-200 °C at unloading was 0.13 wt%. To estimate the total moisture at unloading, an additional 0.04 wt% (1.5 ML) was added to account for chemically adsorbed water that was not removed by heating to 200 °C.

Given the measured RH at unloading of 33.5% at 27.5 °C, the physisorbed moisture of the material at unloading was calculated to be 0.034 wt% (1.2 ML) using BET formalism detailed in Appendix 1. Assuming an additional 1.5 ML (0.04 wt%) present as chemisorbed water, the RH estimate of the moisture on the material at unloading is 0.07 wt%.

Sample unloading and moisture data are summarized in Table 7.

Table 7. Moisture data summary at unloading.

	Parameter	Value	Units
1	Unloading Moisture by LOI-200 °C	0.13	wt%
2	Estimated additional (chemisorbed) moisture present = 1.5 ML	0.04	wt%
3	Estimated total moisture at unloading by LOI = Line 1 + Line 2	0.17	wt%
4	Relative Humidity/Temperature in headspace at unloading	33.5 / 27.5	%/ °C
5	Number of monolayers at unloading RH and temperature using Figure A-1 or Eq. A- and $c=7$	1.2	ML
6	Mass of weakly bound water (RH) using # of MLs in line 5.	0.034	wt%
7	Estimated total moisture at unloading from RH and temperature = line 2 + line 6	0.07	wt%

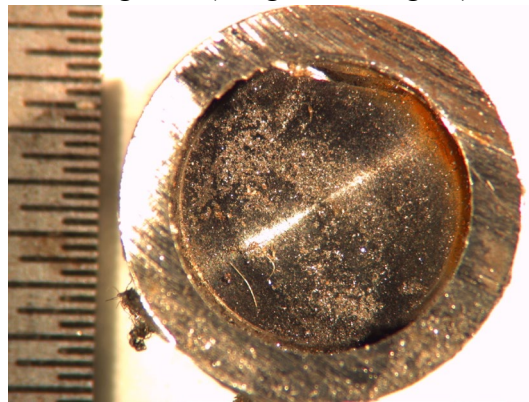
The estimated total moisture at unloading by LOI (0.17 wt%) was approximately 34% of the estimated total moisture at loading by LOI (0.50 wt%).

Corrosion

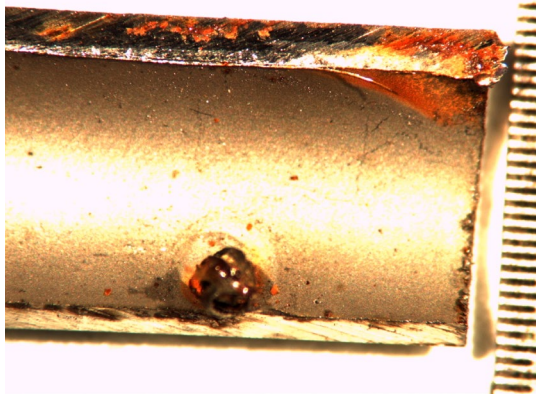
Images of the inner buckets of SSR142 are shown in Figure 8 (images a through h).



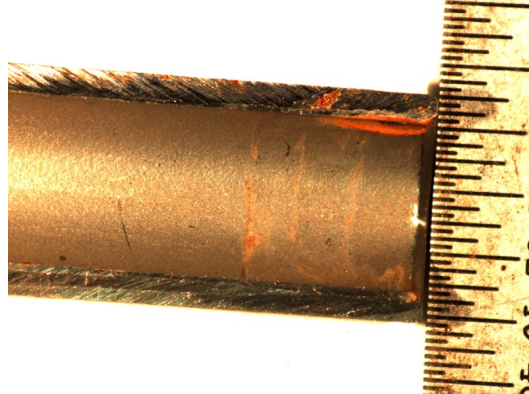
a)



b)



c)



d)

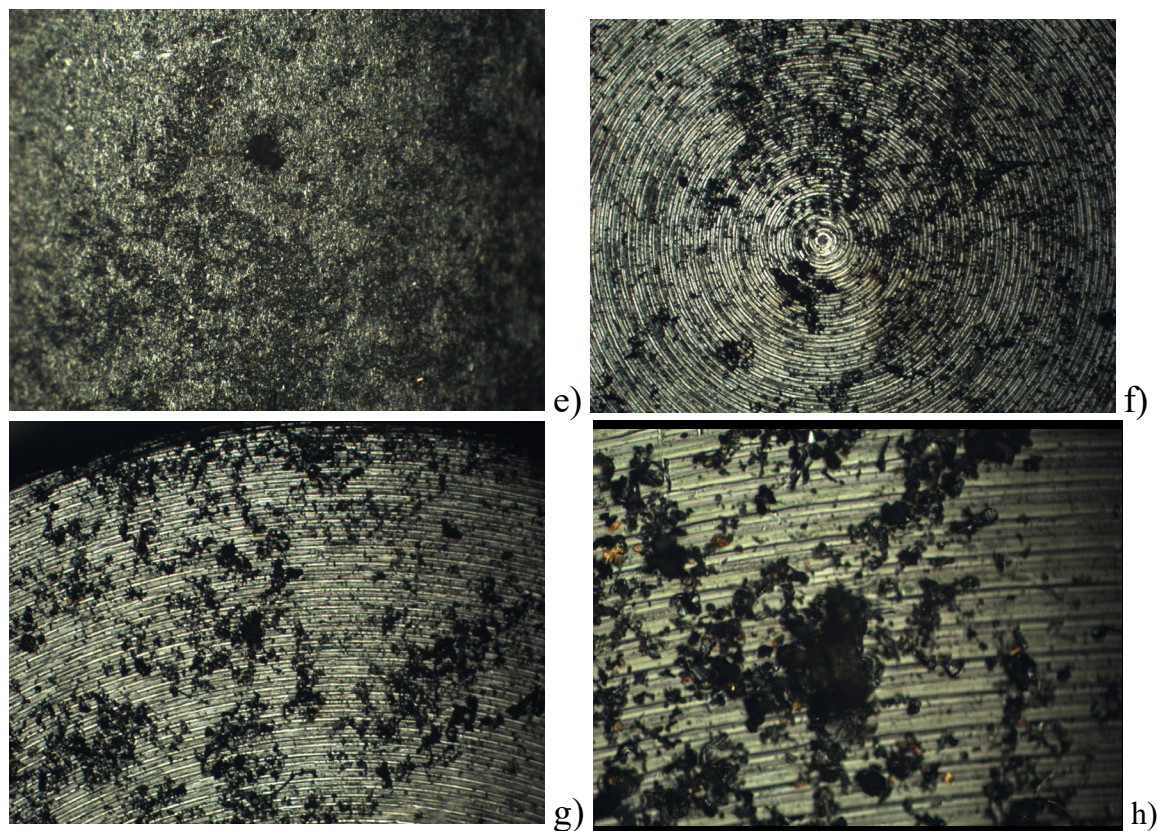


Figure 8. Photographs after unloading: a) inner bucket b) bottom of the inner bucket c), d), & e) possible corrosion inner walls of bucket f) g) & h) bottom of bucket that appeared to be covered with debris.

No significant corrosion was observed on the wall or bottom of the inner bucket. Limited surface corrosion and a possible small pit were observed.

Discussion

A goal of the small-scale surveillance studies is to understand the hydrogen gas generation response of material exposed to moisture over a broad range of materials. Hydrogen partial pressure curves can be analyzed to obtain hydrogen G-values and formation and consumption rate constants assuming that the hydrogen gas is formed either from radiolysis or from surface decomposition of water.⁶ In order to perform these calculations, knowledge of the moisture content of the material during the study and the radiation dose to the moisture is required. We will first discuss the amount of moisture on the material during the study and use the results as input to the $G(H_2)$ and rate constant calculations. We will follow those results with a discussion of the observation of other gases.

A monolayer of hydroxyls forms rapidly when actinide oxide surfaces are exposed to water. Minimal adsorption of atmospheric gases after calcination, such as NO_x and CO_2 , is expected. The observation of CO_2 and NO_x in the TGA-MS is thought to be an artifact of the time between sampling and analysis and are probably due to the radiolysis of plastics that are part of the storage vessel.

The H₂ G-value and rate constants

It is recommended that $G(H_2)$ and rate constants be calculated for materials where H₂ is observed. The mathematical formalism is given in *Obtaining G-values and rate constants from MIS data* and summarized in Appendix 3.⁶ The formation rate constant, k_1 , has been redefined in this report. The hydrogen gas generation rate was determined by fitting the hydrogen partial pressure data as a function of time to Equation 1.

$$P_{H_2}(t) = a(1 - e^{-bt}) \quad \text{Equation 1}$$

This equation is consistent with either a first order formation reaction and no consumption where $a = A_0$ and $b = k_1$

$$P_{H_2}(t) = A_0 (1 - e^{-k_1 t}) \quad \text{Equation 2}$$

or zeroth order formation reaction and a first order consumption reaction where $a = k_1 A_0 / k_2$ and $b = k_2$.

$$P_{H_2}(t) = \frac{k_1 A_0}{k_2} (1 - e^{-k_2 t}) \quad \text{Equation 3}$$

A_0 , the initial active water (water involved in hydrogen gas generation), has units of kPa, and k_1 , the H₂ formation rate constant and k_2 , the H₂ consumption rate constant, have units of day⁻¹. A plot of the fit is shown in Figure 9.

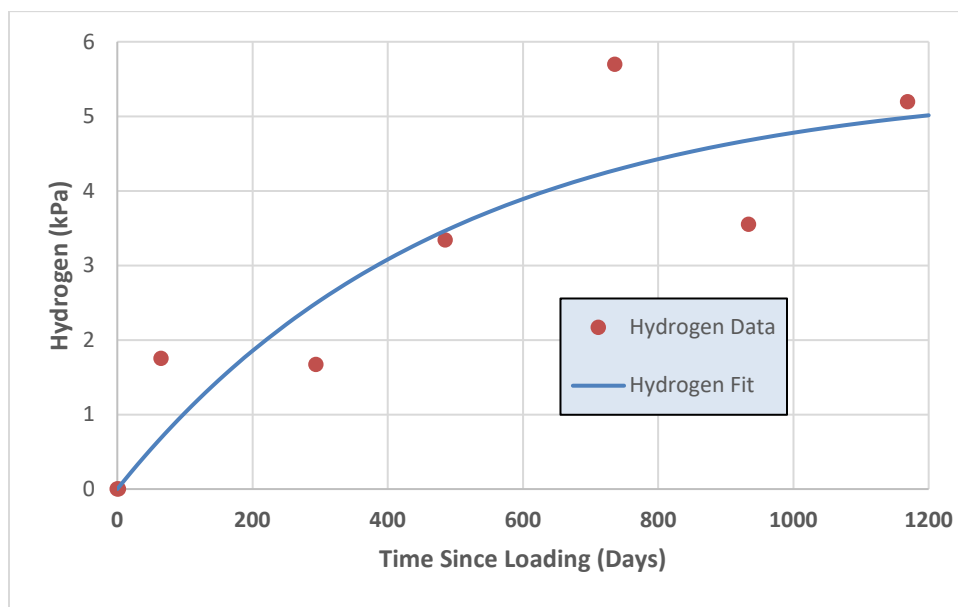


Figure 9. The hydrogen partial pressure and the fit to Equation 1.

The values for the fit parameters a and b that yield the curve in Figure 9 and an r^2 coefficient of 0.79 are given in Table 8. The initial rate was calculated from the product of $a \times b$ as 0.011 kPa/day. The initial hydrogen formation rate can also be approximated from the H₂ partial pressure increase (1.8 kPa) in the first 65 days as 0.028 kPa/day.

Table 8. The fit parameters and standard errors from the hydrogen generation data

SSR sample identification	$a = A_0 k_1/k_2 = P_{max}$	$b = k_2$	$A_0 k_1$
SSR142	5.5 kPa	0.0021 day ⁻¹	0.011 kPa/day
Standard Error	1.7	.001	0.006

The available data do not support a hydrogen generation model of water depletion and hydrogen consumption. An assumption needed for Eq. 3 to be valid is a constant rate of hydrogen generation over the time of the study. That assumption is valid if the water consumed to form hydrogen is small compared to the amount of water available. If the water consumed is small, then the rate of hydrogen formation will be essentially constant and steady state will be established when the rate of formation equals the rate of consumption. The moles of water consumed can be approximated as being equal to the hydrogen formation rate, $A_0 k_1$ (0.011 kPa/day), multiplied by the time the reactor was loaded (1169 days) which is 13 kPa, 0.00038 g or 0.0038 wt%. This amount of water consumed during the study is small compared with the estimated water at loading or the difference in total moisture at loading compared with unloading. Thus, the conditions for Eq. 3 to be valid and a zeroth order formation reaction and a first order consumption reaction are met.

Estimation of the amount of moisture on the material during the gas generation study

Moisture adsorbed on high-purity plutonium dioxide such as PBO-47-09-012-023 is thought to exist as physisorbed (weakly bound) water that behaves according to BET theory⁷ and as chemisorbed (strongly bound) water with very low chemical activity (very low water vapor pressure). The latter water can be described as surface hydroxyls and is removed from the plutonium dioxide surface only at high temperatures. In order to use BET theory to estimate the amount of physisorbed and chemisorbed water on the material during the experiment, the SSA, the amount of water in a monolayer, and the RH are needed. RH data was only available at the termination of the experiment.

The difference between the best estimate of the amount of water in SSR142 when the material was loaded (0.50 wt% from LOI Table 6, line 13) and unloaded (0.07 wt% from RH, Table 7, line 7) is 0.43 wt%. This is much greater than the amount of water that produced H₂ (0.0038 wt%) plus the amount of water that would be in the gas phase at unloading, 0.0003 wt%. A gradual conversion of physisorbed water to chemisorbed water (hydroxyls) during the experiment would contribute to lower measured moisture content at the termination of the experiment but is expected to be approximately 1.5 monolayers (0.04 wt%) of water.^{8, 9}

The major difference is probably due to water condensing in the colder region of the reactor plumbing.⁹ During the gas generation study, the condensed moisture in the cold region of the plumbing is located at a sufficient distance from the material that the radiation dose it receives is orders of magnitude smaller than the radiation dose the water associated with the material receives. This water is NOT expected to contribute to gas generation and would result in a low value for G(H₂) in G-value calculations if it were included in the fraction being subjected to irradiation.

Thus, moisture at loading overestimates the water receiving radiation dose resulting in gas generation since it includes water condensed on the cold region of the reactor. Moisture estimates that include

the 1.5 ML of chemisorbed water may also overestimate water involved in gas generation since it is unlikely the strongly bound water participates. Table 9 summarizes the amount of water on the material, in the gas phase, and decomposed to form H₂ expressed as weight percent, moles, grams, and monolayers.

Table 9. The amount of water adsorbed on the material, in the gas phase, and decomposed to form H₂ expressed as moles, grams, and monolayers. Calculations use SSA = 1.3 m² g⁻¹, m_{mat} = 10.0 g and V_{gas} = 4.391 cm³. The amount of strongly bound chemisorbed water on the material was assumed to be 1.5 monolayers at all times.

Water Source	Amount of Water			
	wt%	g	moles	monolayers
	0.029	0.0029	0.00016	1
Total moisture at loading from Table 6	0.50	0.050	0.0028	17
Water consumed to produce H ₂ (from fit $A_0 k_I = 0.011$ kPa/day)	0.038	0.0038	0.00021	1.3
Water vapor at unloading, 27.5 °C and 33.5% RH (1.2 kPa)	0.0003 (equivalent)	3×10^{-5}	2×10^{-6}	0.01 (equivalent)
Chemisorbed water (1.5 ML)	0.043	0.0043	0.00024	1.5
On material at unloading by RH	0.034	0.0034	0.00019	1.2
Total in system at loading from unloading RH data = water consumed + water vapor + chemisorbed + RH	0.115	0.0115	0.00064	4.0

(Note: Additional moisture could have been consumed in formation of the corrosion products such as iron hydroxide)

$A_0 k_I$ and k_2 are used to calculate $G(H_2)$ and the rate constants for the hydrogen formation and consumption surface reactions using equations in Appendix 3. Because of the uncertainty in determining the amount of water involved in the hydrogen generation, several values are used for the variable m_{H₂O} in Eq. A3-4. The stopping power ratio for PBO-47-09-012-023 material, $\frac{S_{H_2O}}{S_{mat}}$, is 3.7 (Appendix 2). Results for $G(H_2)$ using multiple choices for the amount of water are reported in Table 10 and Table 11.

Table 10. $G(H_2)$ calculated from the reaction parameters and the estimated moisture content using equation A3-4 assuming radiolytic decomposition of water to form H_2 .

Water Source	m_{H_2O}	$G(H_2)$
		molecules $100eV^{-1}$
Total Moisture at Loading from Table 5	0.050 g	0.004
Total moisture at loading from unloading RH data from Table 9	0.0115 g	0.016
Moisture on material at unloading by RH from Table 9	0.0034	0.05

Table 11. Rate constants calculated from the reaction parameters and the estimated initial rate from the fit ($A_0 k_I$) assuming surface catalyzed decomposition of water to form H_2 .

Variable	Equation in Appendix 3	Value	Units
k_{for}	A3-5	1.2E+11	molecules s^{-1}
k_{con}	A3-6	2.2E+10	molecules s^{-1} kPa^{-1}
R_{for}	A3-8	0.057	nanomoles m^{-2} hr^{-1}
R_{con}	A3-9	0.010	nanomoles m^{-2} hr^{-1} kPa^{-1}

Figure 10 illustrates the large differences in $G(H_2)$ depending on the choice of water and compares the $G(H_2)$ values determined in this study with those reported previously.¹⁰

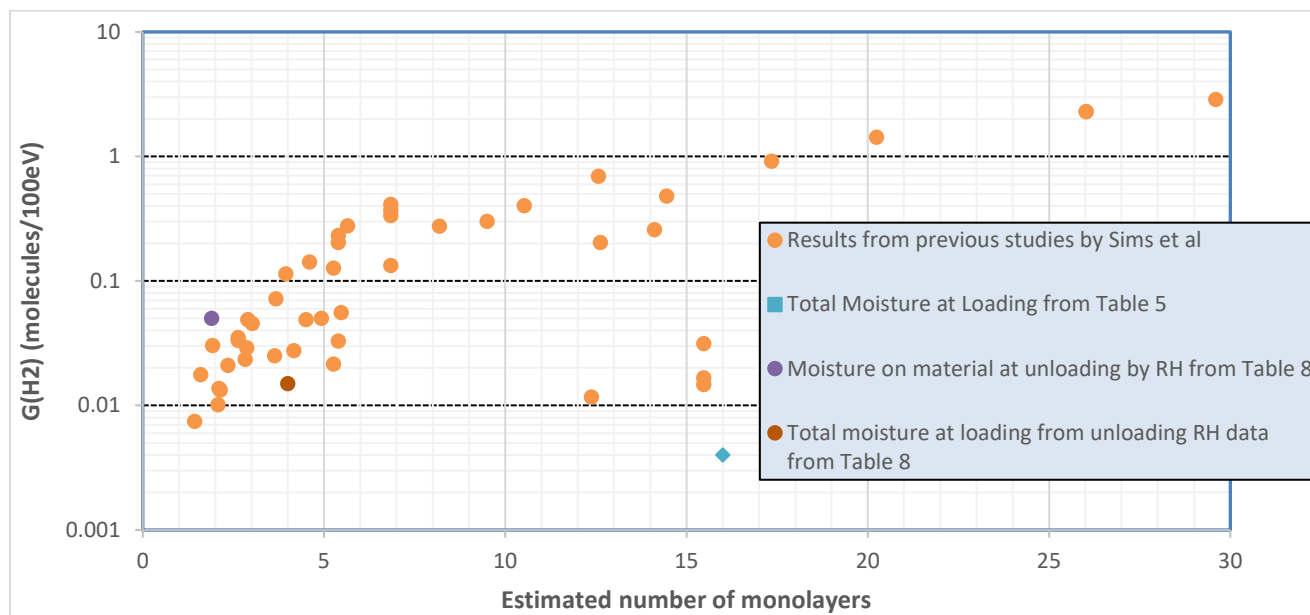


Figure 10. Comparison of calculated $G(H_2)$ plotted against the number of calculated water monolayers determined in this study with those from previous research.

Behavior of NO₂ and CO₂

The 2 kPa of N₂ generated by the material and essentially no CO₂ generated is consistent with the interpretation of the TGA-MS observation of these gases as being formed over the ~3 years the TGA sample was stored before being run. The surface of the material was very clean and contained essentially no adsorbed CO₂ or NO_x.

Behavior of He

The alpha decay of the Pu and Am creates He, which may escape the oxide into the gas phase. The amount of He created depends upon the mass of the material and the rate of decay of the various isotopes. The rate of decay can be illustrated graphically as calculated from the reported isotopics, Figure 3. Results were calculated using the July 29, 1996 isotopics measurements on the AR material that are reported in Table 3. The amount of He created due to alpha decay over the time the material was in the SSR is estimated to be 7×10^{-6} moles for the 10 g sample. This amount of He would result in a gas pressure increase of 4 kPa in the 4.391 ml of gas volume and gas temperature of 328 K, if all the He was released into the gas phase. The seven gas samplings were expected to result in a < 6 kPa decrease in the He pressure. The He pressure decreased by approximately 6.5 kPa by the end of the experiment. (He sampling pressures were somewhat erratic). Results suggest little or no of the He created was released into the gas phase. This analysis does not account for any leaks in the system or the large uncertainties associated with the He gas measurements.

Conclusions

The MIS representative item PBO-47-09-012-023, a high-purity oxide originating in the Hanford continuous oxalate precipitation and calcination process, was entered into surveillance in April of 2003 and removed from surveillance in June of 2007. The amount of water on the material during the gas generation study was estimated to be 0.1 wt%. Gas generation was dominated by H₂ and N₂. Hydrogen was generated to a maximum partial pressure of 5.7 kPa declining to 5.2 kPa at the termination of the experiment. The oxygen that was initially present (0.7 kPa) was consumed. No significant corrosion was observed on the wall or bottom of the inner bucket.

Acknowledgements

Funding for this work was provided to the MIS Program by the Assistant Manager for Nuclear Materials Stabilization, Savannah River Operations Office, Department of Energy's Office of Environmental Management.

References

1. Department of Energy *Stabilization, Packaging, and Storage of Plutonium-Bearing Materials*; DOE-STD-3013-2018; U.S. Department of Energy: Washington, D.C. 20585, 2018.
2. Narlesky, J. E.; Peppers, L. G.; Friday, G. P. *Complex-Wide Representation of Material Packaged in 3013 Containers*; LA-14396; Los Alamos National Laboratory: Los Alamos, NM, 2009.
3. Veirs, D. K.; Worl, L. A.; Harradine, D. M.; Martinez, M. A.; Lillard, S.; Schwartz, D. S.; Puglisi, C. V.; Padilla, D. D.; Carrillo, A.; McInroy, R. E.; Montoya, A. R. *Gas generation and corrosion in salt-containing impure plutonium oxide materials: Initial results for ARF-102-85-223*; LA-UR-04-1788; Los Alamos National Laboratory: Los Alamos, NM, 2004.
4. Veirs, D. K.; Stroud, M. A.; Berg, J.; Narlesky, J. Worl, L.; Martinez, M.; Carillo, A. *MIS High-Purity Plutonium Oxide Metal Oxidation Product TS707001 (SSR123): Final Report*; LA-UR-17-27172; Los Alamos National Laboratory: Los Alamos, NM, 2017.
5. Veirs, D. K.; Berg, J. M.; Crowder, M. L. *The effect of plutonium dioxide water surface coverage on the generation of hydrogen and oxygen*; LA-UR-12-22377; Los Alamos National Laboratory: Los Alamos, NM, 2012.
6. Veirs, D. K.; Berg, J. M.; Stroud, M. A. *Obtaining G-values and rate constants from MIS data*; LA-UR-17-23787; Los Alamos National Laboratory: Los Alamos, NM, 2017.
7. Brunauer, S.; Emmett, P. H.; Teller, E., Adsorption of Gases in Multimolecular Layers. *Journal of the American Chemical Society* **1938**, 60.
8. Veirs, D. K.; Berg, J. M.; Hill, D. D.; Harradine, D. M.; Narlesky, J. E.; Romero, E. L.; Trujillo, L.; Wilson, K. V. *Water radiolysis on plutonium dioxide: Initial results identifying a threshold relative humidity for oxygen gas generation*; LA-UR-12-26423; Los Alamos National Laboratory: Los Alamos, NM, 2012.
9. Veirs, D. K. S., M. A.; Martinez, M.; Carrillo, A.; Berg, J.; Narlesky, J.; Worl, L. *MIS High-Purity Plutonium Oxide Metal Oxidation Product TS707001 (SSR123): Final Report*; LA-UR-17-27172; Los Alamos National Laboratory: Los Alamos, NM, 2017.
10. Sims, H. E. W., K. J.; Brown, J.; Morris, D.; Taylor, R. J., Hydrogen yields from water on the surface of plutonium dioxide. *Journal of Nuclear Materials* **2013**, (437), 359-364.
11. Haschke, J. M.; Ricketts, T. E., Adsorption of water on plutonium dioxide. *Journal of Alloys and Compounds* **1997**, 252, 148-156.
12. (a) Haschke, J. M.; Allen, T. H.; Morales, L. A., Reaction of Plutonium Dioxide with Water: Formation and Properties of PuO_{2+x} . *Science* **2000**, 287, 285-286; (b) Haschke, J. M.; Allen, T. H.; Morales, L. A., Reactions of plutonium dioxide with water and hydrogen–oxygen mixtures: Mechanisms for corrosion of uranium and plutonium. *Journal of Alloys and Compounds* **2001**, 314, 78-91.

Attachment 1: Gas Generation Partial Pressure Data and Uncertainties in kPa

(Page 1 of 1)

Note: Total pressure values used to determine partial pressures were reduced by 4kPa to correct for the estimated partial pressure of water vapor. Partial pressures were corrected for variation in the sensitivity of the GC with time. The average manifold background pressure was subtracted from the partial pressures.

Date	4/7/2004	6/9/2004	1/24/2005	8/3/2005	4/11/2006	10/26/2006	6/18/2007
Days	2.0	65.0	294.0	485.0	736.0	934.0	1169.0
CO ₂	0.5	0.6	0.0	0.0	0.0	0.0	0.0
N ₂ O	0.0	0.0	0.0	0.0	0.0	0.0	0.0
He	84.8	80.1	78.4	78.7	81.2	76.9	78.3
H ₂	0.0	1.8	1.7	3.3	5.7	3.6	5.2
O ₂	0.7	0.4	0.3	0.0	0.0	0.0	0.1
N ₂	2.2	3.7	4.6	4.2	3.5	2.9	2.8
CH ₄	0.0	0.0	0.0	0.0	0.0	0.0	0.0
CO	0.0	0.0	0.0	0.1	0.1	0.2	0.2
H ₂ O (estimate)	4	4	4	4	4	4	4
Total Pressure	92.2	90.5	88.8	90.2	94.6	87.4	90.5

Uncertainties

Date	4/7/2004	6/9/2004	1/24/2005	8/3/2005	4/11/2006	10/26/2006	6/18/2007
Days	2.0	65.0	294.0	485.0	736.0	934.0	1169.0
CO ₂	0.03	0.02	0.01	0.00	0.00	0.00	0.00
N ₂ O	0.00	0.00	0.00	0.00	0.00	0.00	0.00
He	1.74	1.65	1.61	1.62	1.67	1.58	1.61
H ₂	0.00	0.04	0.04	0.07	0.12	0.08	0.11
O ₂	0.03	0.02	0.01	0.00	0.00	0.01	0.01
N ₂	0.07	0.09	0.11	0.10	0.09	0.08	0.08
CH ₄	0.00	0.00	0.00	0.00	0.00	0.00	0.00
CO	0.00	0.00	0.00	0.01	0.01	0.01	0.02

Attachment 2: Gas Generation: Total Pressure

(Page 1 of 2)

Date	Pressure (kPa)	Date	Pressure (kPa)	Date	Pressure (kPa)	Date	Pressure (kPa)	Date	Pressure (kPa)
4/5/2004	91.70	8/9/2004	89.94	12/20/2004	89.04	4/25/2005	91.0	8/29/2005	92.8
4/12/2004	92.96	8/16/2004	89.48	12/27/2004	89.93	5/2/2005	91.7	9/5/2005	93.3
4/19/2004	93.11	8/23/2004	89.02	1/3/2005	89.90	5/9/2005	91.1	9/12/2005	92.5
4/26/2004	93.93	8/30/2004	89.77	1/10/2005	89.72	5/16/2005	90.9	9/19/2005	93.2
5/3/2004	94.54	9/6/2004	89.52	1/17/2005	90.41	5/23/2005	90.7	9/26/2005	93.7
5/10/2004	93.21	9/13/2004	88.73	1/24/2005	90.03	5/30/2005	90.8	10/3/2005	92.80
5/17/2004	92.62	9/20/2004	88.97	1/31/2005	86.90	6/6/2005	90.6	10/10/2005	92.58
5/24/2004	91.78	9/27/2004	89.49	2/7/2005	87.12	6/13/2005	90.9	10/17/2005	93.61
5/31/2004	91.89	10/4/2004	89.63	2/14/2005	86.51	6/20/2005	91.3	10/24/2005	93.67
6/7/2004	91.02	10/11/2004	88.94	2/21/2005	86.44	6/27/2005	88.9	10/31/2005	94.98
6/14/2004	89.58	10/18/2004	88.50	2/28/2005	86.88	7/4/2005	87.8	11/7/2005	94.35
6/21/2004	88.11	10/25/2004	89.05	3/7/2005	88.44	7/11/2005	87.3	11/14/2005	94.66
6/28/2004	88.91	11/1/2004	88.79	3/14/2005	88.78	7/18/2005	87.6	11/21/2005	96.53
7/5/2004	88.51	11/8/2004	89.79	3/21/2005	89.71	7/25/2005	90.1	11/28/2005	95.59
7/12/2004	89.23	11/15/2004	89.15	3/28/2005	90.97	8/1/2005	91.4	12/5/2005	96.57
7/19/2004	89.65	11/22/2004	88.86	4/4/2005	91.36	8/8/2005	89.6	12/12/2005	94.92
7/26/2004	90.05	11/29/2004	89.18	4/11/2005	91.4	8/15/2005	90.7	12/19/2005	94.91
8/2/2004	89.53	12/6/2004	88.69	4/18/2005	91.6	8/22/2005	92.1	12/26/2005	94.21

Attachment 2: Gas Generation: Total Pressure

(Page 2 of 2)

Date	Pressure (kPa)	Date	Pressure (kPa)	Date	Pressure (kPa)	Date	Pressure (kPa)	Date	Pressure (kPa)
1/2/2006	94.49	5/8/2006	94.65	9/11/2006	91.16	1/15/2007	89.753094	5/21/2007	91.166481
1/9/2006	94.54	5/15/2006	96.13	9/18/2006	90.92	1/22/2007	89.958059	5/28/2007	91.53606
1/16/2006	91.26	5/22/2006	95.18	9/25/2006	91.36	1/29/2007	89.937873	6/4/2007	92.122048
1/23/2006	90.91	5/29/2006		10/2/2006	90.63	2/5/2007	90.903223	6/11/2007	92.015217
1/30/2006	91.73	6/5/2006	95.32	10/9/2006	90.51	2/12/2007	89.550935	6/18/2007	91.849542
2/6/2006	93.36	6/12/2006	95.13	10/16/2006	87.336526	2/19/2007	89.965542		
2/13/2006	92.41	6/19/2006	94.94	10/23/2006	88.535708	2/26/2007	90.283084		
2/20/2006	90.75	6/26/2006	95.00	10/30/2006	86.734717	3/5/2007	91.977751		
2/27/2006		7/3/2006	93.88	11/6/2006	87.133658	3/12/2007	91.417073		
3/6/2006		7/10/2006	92.88	11/13/2006	80.037375	3/19/2007	91.169869		
3/13/2006		7/17/2006		11/20/2006	87.670069	3/26/2007	91.220678		
3/20/2006		7/24/2006	92.02	11/27/2006	87.008863	4/2/2007	91.306126		
3/27/2006		7/31/2006	91.67	12/4/2006	88.674113	4/9/2007	90.70737		
4/3/2006		8/7/2006	92.02	12/11/2006	87.817234	4/16/2007	91.125355		
4/10/2006	95.30	8/14/2006	89.18	12/18/2006	88.600708	4/23/2007	91.413516		
4/17/2006	96.26	8/21/2006	91.70	12/25/2006	89.609404	4/30/2007	91.639494		
4/24/2006	94.15	8/28/2006	91.18	1/1/2007	89.272155	5/7/2007	92.095627		
5/1/2006	94.25	9/4/2006	91.57						

Appendix 1: Estimating the monolayer coverage

(Page 1 of 2)

Surface Area: The number of monolayers of moisture on the sample surface may be calculated if the mass of moisture or water, the mass of the sample, and the SSA of the sample are known. One approach is to determine the weight percentage for one monolayer of water. The number of monolayers of water can be calculated by dividing the total weight percentage of water (mass of water/mass of the sample) by the weight percentage of one monolayer of water.¹¹ The weight percentage of one monolayer of water is the product of the weight of water in a monolayer of 1 m² and the SSA:

$$\begin{aligned}\text{wt\% of 1 ML} &= 0.00022 \text{ g m}^{-2}\text{ML}^{-1} \times \text{SSA m}^2 \text{ g}^{-1} \times 100 \text{ wt\%} \\ &= 0.022 \text{ wt\% ML}^{-1} \times \text{SSA.}\end{aligned}\quad \text{Equation A1-1}$$

For the material with a SSA of 1.30 m² g⁻¹, the weight percentage of one monolayer of water is 0.029 wt% ML⁻¹.

Dividing the weight percentage of water by the weight percentage of water in one monolayer yields the number of monolayers of water. Applying this to the measured weight percentage of water upon loading and unloading results in:

$$\text{Loading Condition:} \quad 0.50 \text{ wt\%} / 0.0286 \text{ wt\% ML}^{-1} = 17 \text{ ML}$$

$$\text{Unloading Condition:} \quad 0.07 \text{ wt\%} / 0.0286 \text{ wt\% ML}^{-1} = 2.4 \text{ ML}$$

BET Theory: The number of monolayers can also be estimated based upon the relative humidity in the container using Brunauer-Emmett-Teller (BET) theory.⁷ BET theory is the standard model for quantifying the equilibria between multiple physically adsorbed layers on a surface and the adsorbing species in the gas above the surface. The specific relationship between the RH above a surface and the number of monolayers of weakly bound water on the surface predicted by BET theory is illustrated in Fig. A1-1.

Appendix 1: Estimating the monolayer coverage

(Page 2 of 2)

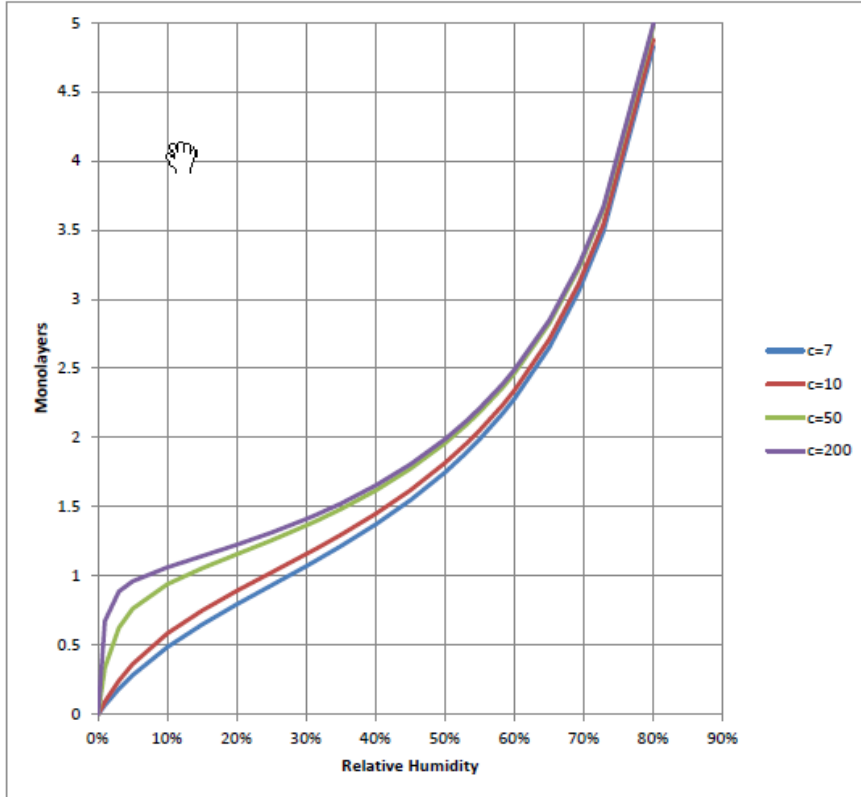


Figure A1-1. Adsorption Isotherm Calculated from BET Theory.

The equation for calculating the number of monolayers at a given RH and c value is given in Equation A1-2.

$$ML = \frac{c \frac{RH}{100\%}}{\left(1 - \frac{RH}{100\%}\right) \left(1 + (c - 1) \frac{RH}{100\%}\right)}$$

Equation A1-2

Appendix 2: Stopping power ratio

(Page 1 of 1)

The ratio of the stopping power due to the water and the stopping power due to the material is calculated using the approach in Appendix B of Reference 6. Elements with greater than 0.3 wt% were included.

Element or Compound	Integrated Stopping Power from 0 to 5.2 MeV (mg ⁻¹ cm ⁻²)	Elemental Mass Fraction	Elemental Stopping Power (mg ⁻¹ cm ⁻²)
H2O(g)	7.946	0.0000	0
H2O (l)	7.708	0.0067	0.052
F	6.645	0.0000	0
O	5.901	0.0000	0
Na	5.304	0.0000	0
C	5.190	0.0000	0
S	5.117	0.0000	0
Mg	5.100	0.0000	0
Si	4.852	0.0000	0
Al	4.702	0.0000	0
K	4.652	0.0000	0
Cl	4.575	0.0000	0
Ca	4.461	0.0000	0
Cr	3.688	0.0000	0
Fe	3.504	0.0000	0
Ni	3.184	0.0000	0
Cu	2.871	0.0000	0
Zn	2.860	0.0000	0
Ga	2.786	0.0000	0
UO2	2.081	0	0
PuO2	2.081	0.999	2.08
		Smat	2.08
		Swat	7.71
		S	3.70

Appendix 3: Obtaining G-values and rate constants

(Page 1 of 3)

As discussed in the H₂ G-value section, a three-exponential function (Eq. 5) was used to fit the time dependence of the partial pressure curve for hydrogen for SSR142. The function has fitting parameters, A₀, the initial water involved in hydrogen generation and k₁ the hydrogen formation rate constant can be used along with information of material properties and container geometry to calculate the initial rate, the hydrogen G-value. This appendix documents the methodology for obtaining this information.

Calculation of G(H₂)

G(H₂) can be calculated by equating the initial rate of hydrogen generation to the product of the rate of radiation dose to the water and G(H₂),

$$\frac{dN_{H_2}}{dt} = \dot{D}_{H_2O} G(H_2) \quad \text{Equation A3-1}$$

where N_{H2} is the number of molecules of hydrogen and \dot{D}_{H_2O} is the rate of adsorbed dose to the water with units eV s⁻¹. The initial rate evaluated at time zero in units of molecules per second rather than kPa per day.

$$\begin{aligned} \left. \frac{dP}{dt} \right|_{t=0} &= k_1 A_0 \\ \frac{dN_{H_2}}{dt} &= \frac{dP}{dt} \frac{V_g N_A}{R T} = k_1 A_0 \frac{V_g N_A}{R T} \frac{\text{day}}{86400 \text{ s}} \\ k_1 A_0 \frac{V_g N_A}{R T} \frac{\text{day}}{86400 \text{ s}} &= \dot{D}_{H_2O} G(H_2) \end{aligned} \quad \text{Equation A3-2}$$

In Equation A3-2, V_g is the gas volume within the reactor, N_A is Avogadro's number, R is the universal gas constant, T is the temperature in the gas phase during the time the data was collected. The method for calculating V_g within an SSR is shown in the Loading section. The dose rate to the water is given by

Appendix 3: Obtaining G-values and rate constants

(Page 2 of 3)

$$\begin{aligned}\dot{D}_{H_2O} &= P_{mat} \frac{6.2418 \times 10^{18} \text{ eV}}{\text{s W}} m_{mat} f_{H_2O} \frac{S_{H_2O}}{S_{mat}} \\ f_{H_2O} &= \frac{m_{H_2O}}{m_{mat}} \\ \dot{D}_{H_2O} &= P_{mat} \frac{6.2418 \times 10^{18} \text{ eV}}{\text{s W}} m_{H_2O} \frac{S_{H_2O}}{S_{mat}}\end{aligned}\quad \text{Equation A3-3}$$

where P_{mat} is the specific power of the material in W g^{-1} , m_{mat} is the mass of the material, f_{H_2O} is the mass fraction of water, and the ratio S_{H_2O}/S_{mat} is the ratio of the stopping power of alpha particles in water to the stopping power in the material. An approach for calculating S_{H_2O}/S_{mat} is given in Appendix 2. For high-purity plutonium dioxide with adsorbed water and no impurities the ratio S_{H_2O}/S_{mat} for 5.2 MeV α -particles is ~ 3.70 . Combining Equation A3-2 and A3-3 yields a general expression for $G(H_2)$ using $A_0 k_I$ (determined from the fitting parameters a and b of Eq.1) and the material properties,

$$G(H_2) = k_1 A_0 \frac{V_g N_A}{R T} \frac{\text{day}}{86400 \text{ s}} \frac{1}{P_{mat} \frac{6.2418 \times 10^{18} \text{ eV/100}}{\text{s W}} m_{H_2O} \frac{S_{H_2O}}{S_{mat}}} \frac{1}{\frac{S_{H_2O}}{S_{mat}}}. \quad \text{Equation A3-4}$$

Conversion of rate constants

The initial formation rate constant, k_{for} , can be expressed in terms of molecules of hydrogen produced per second of active water using the equations below.

$$k_{for} = k_1 A_0 \frac{V_g N_A}{R T} \frac{\text{day}}{86400 \text{ s}} \quad \text{Equation A3-5}$$

The consumption rate constant, k_2 , expressed in units of days^{-1} , can be expressed in terms of molecules of hydrogen consumed per second per kPa of hydrogen using the equations below.

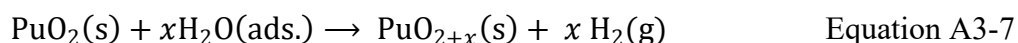
$$k_{con} = k_2 \frac{V_g N_A}{R T} \frac{\text{day}}{86400 \text{ s}} \quad \text{Equation A3-6}$$

Appendix 3: Obtaining G-values and rate constants

(Page 3 of 3)

Calculation of rate constants for surface catalyzed decomposition of water to form H₂

The surface catalyzed decomposition of water to form H₂ has been proposed by Haschke and co-workers.¹² The reaction is described by,



The reaction “contributes to H₂ pressurization of sealed storage containers until the equilibrium pressure of Equation A5-7 is reached.”^{12a} The amount of solid plutonium dioxide and water is large compared to the amount of H₂ and higher oxide produced. The initial reaction rate will be essentially constant throughout the reaction. The H₂ consumption reaction, in this case a true back reaction, is first order in H₂ partial pressure and in the amount of the higher oxide. The rate was found to be independent of adsorbed water over a wide range of adsorbed water. The observed initial rate of formation is divided by the total surface area of the material to obtain values that can be compared to Haschke’s reaction rates,

$$R_{for} = A_0 k_1 \frac{\text{day}}{24 \text{ hr}} \frac{V_g}{R T} \frac{1}{SSA m_{mat}} \quad \text{Equation A3-8}$$

where SSA is the specific surface area of the material and m_{mat} is the mass of the plutonium dioxide. This formation rate, R_{for} , is expressed in units of moles m⁻² hr⁻¹ kPa⁻¹ of active water. The rate of the surface catalyzed consumption reaction is given by

$$R_{con} = k_2 \frac{\text{day}}{24 \text{ hr}} \frac{V_g}{R T} \frac{1}{SSA m_{mat}} \quad \text{Equation A3-9}$$

Appendix 4: Symbols and Conversion Factors

(Page 1 of 2)

Symbols

Symbol	Units	Description
A	kPa	Water involved in hydrogen generation
A_0	kPa	Initial water involved in hydrogen gen (fitting parameter)
k_1	day ⁻¹	Rate constant for the formation of hydrogen from water (fitting parameter)
k_2	day ⁻¹	Rate constant for the consumption of hydrogen (fitting parameter)
k_3	day ⁻¹	Rate constant for the back reaction formation of hydrogen (fitting parameter)
\dot{D}_x	eV s ⁻¹ or J s ⁻¹ or W	Rate of adsorbed dose to x
$G(x)$	molecules 100 eV ⁻¹	Number of molecules of x produced per 100 eV of adsorbed dose
f_x	---	Fraction of material x in the total material
m_x	g	Mass of x
N_x	molecules	Number of molecules of substance x
N_A	molecules mol ⁻¹	Avogadro's number
p_x	kPa	Partial pressure of x
P_x	W g ⁻¹ or eV s ⁻¹ g ⁻¹	Specific power of x
S_x	m	Stopping power of x to alpha radiation
SSA	m ² g ⁻¹	Specific Surface Area of the material
t	s or day or yr	Time
T	K	Temperature
V_g	cm ³	Volume that the gas occupies

Appendix 4: Symbols and Conversion Factors

(Page 2 of 2)

Unit conversions

1 W	$6.2418 \times 10^{18} \text{ eV s}^{-1}$
1 day	86400 s
1 day	24 hr
N_A	$6.0221367 \times 10^{23} \text{ molecules mol}^{-1}$
R	$8.314510 \text{ J mol}^{-1} \text{ K}^{-1}$ $8.314510 \text{ kPa L mol}^{-1} \text{ K}^{-1}$ $8314.510 \text{ kPa cm}^3 \text{ mol}^{-1} \text{ K}^{-1}$